MEASUREMENTS OF THERMAL IMPEDANCE ON SUPERCONDUCTING RADIOFREQUENCY CAVITIES*

Pashupati Dhakal†, Gianluigi Ciovati and Ganapati Rao Myneni
Jefferson Lab, Newport News, VA 23606, USA

Abstract

The thermal impedance of niobium plays an important role in the thermal stability of the superconducting radio frequency (SRF) cavities used in particle accelerators. During the operation of SRF cavities, the RF power dissipates on the inner surface of the cavities and the heat transport to the helium bath depends on the thermal conductivity of niobium and Kapitza conductance at the interface between the niobium and superfluid helium. Thermal impedance was measured on three 1.3 GHz single cell cavities made from ingot niobium with different purity. The results show the influence of surface preparation on thermal impedance and the results are qualitatively in agreement to the power law dependence with temperature as reported in the literature.

INTRODUCTION

Superconducting radio frequency cavities are the building blocks of particle accelerators for basic physics research. It is based on niobium superconducting hollow structures ("cavities") to accelerate the beam of charged particles to the velocity of light. The superiority of superconducting material is its ability to efficiently store large amount of energy with no or very little dissipation. The performance of SRF cavities is measured in terms of the quality factor expressed as $Q_0 = \omega U/P$, where U is stored energy and (P/ω) is the power dissipation on inner cavity wall per rf cycle. Ideally, the quality factor of SRF cavities is independent of the accelerating field (or peak magnetic field) as the breakdown occurs at superheating field. However, due to the finite resistance of the superconductor in rf field, power dissipates on the cavity walls due to the interaction of the rf field with normal conducting electrons. At high peak magnetic field the dissipation is believed to be of magnetic origin, where the surface resistance increases due to pair-breaking by the increasing rf field gives rise to the non-linear BCS surface resistance [1]. The cavity then goes to the magneto-thermal instability and finally "quench". The dissipated power is given by $P_{diss} = (1/2\mu_0)R_s(T)B_p^2$, where μ_0 is magnetic permeability, $R_s(T)$ is surface resistance, and B_p is peak rf magnetic field on the inner surface of the cavity.

The power dissipated (heat) on the inner surface of SRF cavities during the operation is conducted through the cavity wall into the helium bath. The efficient transport of heat from the inner cavity wall to the helium bath depends on the thermal conductivity of niobium and the Kapitza conductance between the outer cavity surface and the superfluid helium. The thermal conductivity of niobium is material dependent, for example the impurities contents (related to the residual resistivity ratio-RRR), crystal grain sizes, mechanical deformation, defects and dislocations in niobium. The Kapitza resistance is an intrinsic thermal resistance due to the phonon mismatch at the boundary between Nb and the superfluid He and depends on the nature of solid surface. In this contribution, we present some preliminary results in an attempt to understand the effect of surface preparations on the thermal resistance on SRF cavities.

EXPERIMENTAL SETUP

Previously, thermal impedance measurements on SRF niobium samples were carried out in an experimental cell which allows us to measure the thermal conductivity and Kapitza resistance [2–4] by measuring the temperature jump across the niobium samples. Palmieri *et al.*, [5] measured the thermal boundary resistance via the rf surface resistance measurement in SRF cavities and showed the change in thermal boundary resistance as the outer surface of cavity was modified. In our present study, we have estimated the thermal impedance of SRF cavity using the method used in refs. [2,3]. The schematic representation of the experimental set up is shown in Fig. 1.

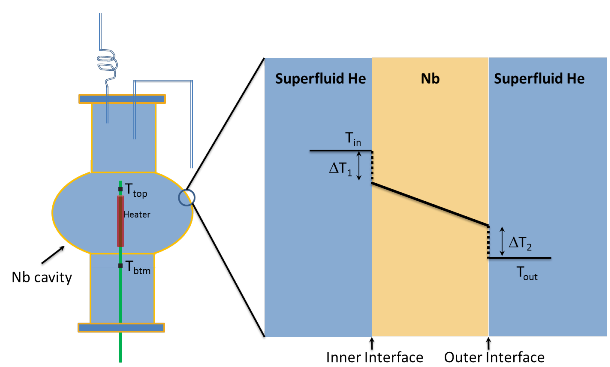

Figure 1: Schematic of experimental set up.

Niobium SRF cavity of thickness ∼ 2.9 mm is immersed in superfluid helium bath and filled with superfluid He via a capillary tube of diameter ∼1.5mm. Two capillary tubes are used, one for filling and other for exhaust to He gas during filling , welded to a ∼ 9.5mm thick stainless steel flange sealed to one cavity flange with indium wire. A cryogenic heater of resistance ∼8.5 Ω is inserted along the axis of the cavity using a G10 rod. Two calibrated thermometers are attached at the both ends of the G10 rod, measuring the

* This manuscript has been authored by Jefferson Science Associates, LLC under U.S. DOE Contract No. DE-AC05-06OR23177. The U.S. Government retains a non-exclusive, paid-up, irrevocable, world-wide license to publish or reproduce this manuscript for U.S. Government purposes.
† dhakal@jlab.org

temperature at the middle of cavity and on the beam tube. The outside temperature is regulated via He pumping and the temperature is held to within ± 1 mK. In the absence of any heat the superfluid He inside the cavity is in thermal equilibrium with the bath temperature. The temperature rise inside the cavity is measured as a function of the applied power as shown in Fig. 2(a). Due to the high thermal conductivity of the superfluid helium, thermal equilibrium is achieved and the power density on the inner cavity surface is assumed to be uniform. The surface area of the single cell cavity is ~1486 cm^2 including the beam tubes and ~153 cm^2 consists of stainless steel. With the thermal conductivity of stainless steel at 2K of ~ 0.1 W/m K [6], the total heat loss through the flanges is estimated to be less than 2 %. The critical heat flux through the capillary tube varies with temperature from 1.5K to the lambda point, between ~ 80-180 mW/cm^2, with a maximum ~ 1.7 K [7]. In our experimental setup, the maximum heat loss via superfluid helium is estimated to be less than 2%. The heat loss via the electrical feedthrough is negligible. Thus ~ 96 % of heat was carried away across the cavity including the beam tubes. Beam tubes were made from the low purity reactor grade niobium and thermal conductivity at 2K is ~ 1 W/m K [8]. The results presented in this contribution are the combined effect for both beamtubes and cavity.

Under the steady state condition, the temperature jump $\Delta T = T_{in} - T_{out}$ is established. The temperature difference can be written as

$$\Delta T = T_{in} - T_{out} = R_B Q \tag{1}$$

Here, the slope of the curve $\Delta T vs Q$ given by $R_B = \frac{d}{\kappa} + R_K$ is the thermal impedance, where d is the thickness of the wall, κ is the thermal conductivity, R_K represents the thermal resistance between the wall and the superfluid He (Kapitza resistance). The measured thermal impedance is the sum of the contribution from the stainless steel and niobium cavity. Since ~ 96% of heat is carried away across the cavity, the contribution to the thermal impedance due to stainless steel can be neglected. It is to be noted that there are two interfaces (inner and outer surface) between niobium and superfluid He, thus $R_K = R_{K,in} + R_{K,out}$. The unit of the thermal impedence will be $cm^2 K/W$ in the paper.

Table 1: List of the Cavities and Surface Preparations

Cavity ID	RRR	Process
TC1N1	60	as available, EP, BCP
CBMM-A4	280	N2 doping, EP, BCP
TD5	350	N2 doping and EP, BCP

The thermal impedance ($\frac{d}{\kappa} + R_K$) can be estimated from the fit of ΔT vs Q as shown in Fig. 2(b). Three 1.3 GHz single cell cavities with different residual resistivity ratio (RRR) were used in this study to estimate the thermal impedance. The cavity surface is modified with chemical polishing as well as nitrogen doping to understand the effect of surface preparation on the thermal impedance. Table 1 summarizes the list of the cavities and the surface preparations done before the thermal impedance measurements.

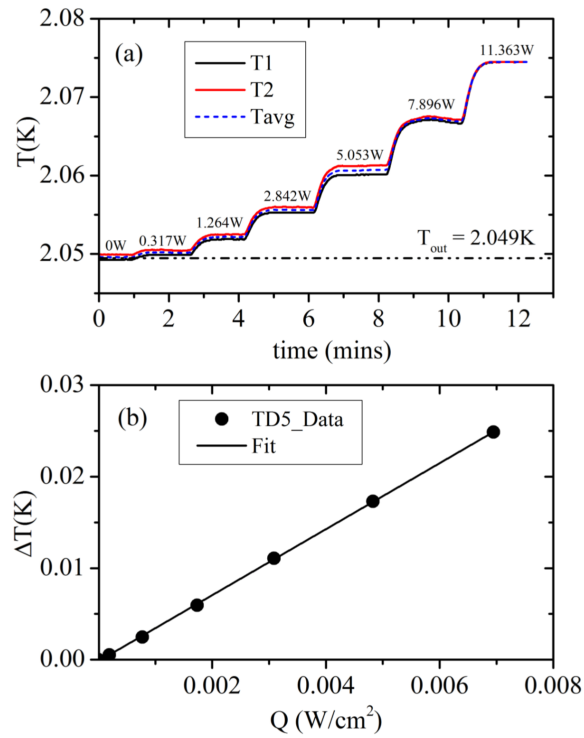

Figure 2: Typical experimental data measured. (a) The increase in temperature of superfluid He inside the cavity as a function of applied power at 2.05 K and (b) the plot of ΔT vs Q for cavity TD5. The slope of the fit gives the thermal impedance at 2.05 K.

EXPERIMENTAL RESULTS

TC1N1

TC1N1 is Tesla shape single cell cavity made from low purity ingot niobium. After the fabrication with electron beam welding the cavity's inner surface was barrel polished ~60μm followed by electropolishing ~30 μm, heat treatment at 800 °C/3hrs and additional electropolishing of ~15μm. Before the heat treatment the outside surface of cavity was buffer chemical polished (BCP) ~20μm to remove impurities from the outer surface. The thermal impedance was measured after an additional EP of ~30μm removal from inner surface and ~13μm additional outside BCP before the final test. In this particular cavity, The thermal conductivity was measured by Fourier method [9] in a sample cut from the original ingot [9]. The sample was BCP and heat treated at 800 °C/3hrs. A high phonon peak ~ 1.8K is observed with very high thermal conductivity as shown in Fig. 3(a). Even though the mechanically deformed SRF cavity may have different thermal conductivity, we have used this measured thermal conductivity to estimate the Kapitza resistance

ISBN 978-3-95450-178-6

for cavity TC1N1 as shown in Fig. 3(b). The data are fitted with a power law and found to be $R_k = 65.5T^{-3.64}$ for cavity initially fabricated (□). After an additional 30 μm EP (○), the temperature dependence is $R_k = 74.5T^{-3.64}$ and after an outside BCP (△) the dependence is $R_k = 94.4T^{-3.79}$. The Kapitza resistance is higher than that measured in samples [2, 3], possibly due to the over estimation of thermal conductivity in mechanically deformed cavity. However, the temperature dependence of Kapitza resistance is in agreement with earlier measurements [2, 3] and theoretical predictions of $R_K \sim T^{-n}$, where $n \sim 2.0$-4.5 [10].

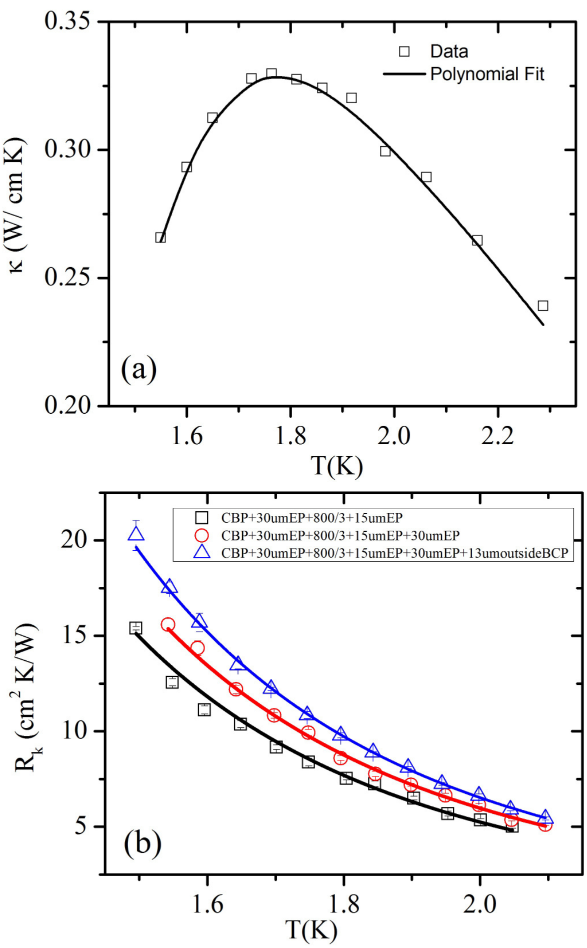

Figure 3: (a) The thermal conductivity of the sample cut out from the same ingot that was used to fabricate the cavity TC1N1. Also shown is a polynomial fit of the experimental data. The sample was subjected to the BCP to remove the damage layer and followed by the heat treatment at 800 °C for 3 hours. (b) The estimated Kapitza resistance measured in cavity TC1N1 after the initial fabrication (□),30 μm, additional inside EP (○) and 13 μm outside BCP (△).

CBMM-A4

CBMM-A4 is single cell cavity made from ingot niobium from CBMM. After the fabrication, the cavity went to several steps of heat treatments and BCP. Before the thermal impedance measurements the cavity was subjected to heat

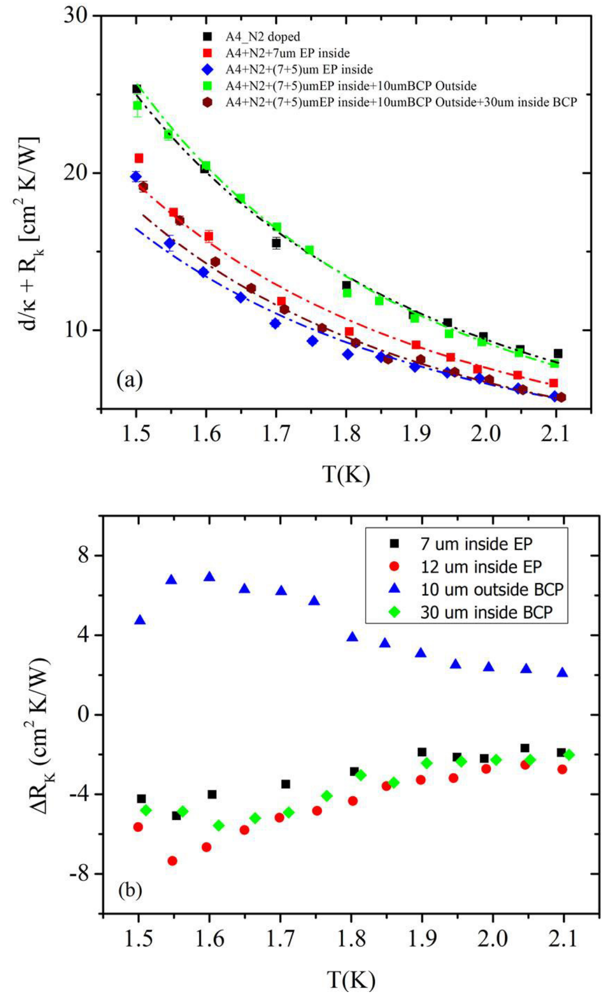

Figure 4: (a)Results of the thermal impedance measurement on cavity CBMM-A4 after the surface preparation as described in text. (b) The change in Kapitza resistance on SRF cavity after different surface modification assuming the thermal conductivity remains unchanged during the surface preparation.

treatment at 800 °C/3hrs followed by 2 minutes pure nitrogen injection with pressure ~ 25 mtorr. After 2 minutes, the nitrogen was evacuated from the furnace and the cavity was further annealed for 10 mins. This process is recently developed [11] and applied to ingot niobium cavities to achieve higher quality factor [12,13]. The details of the rf test done in this cavity will be presented in future contributions. Figure 4(a) shows the results of the measurements after the cavity was subjected to the several surface treatments. The surface preparation with nitrogen doped cavity and inside EP and outside BCP surfaces have very close thermal impedance. The experimental results were fitted with the power law and found $R_B = 98.9T^{-3.39}$ for nitrogen doped surface, $R_B = 72.3T^{-3.24}$ for 7μm inside EP, $R_B = 59.4T^{-3.24}$ for additional 7μm inside EP, $R_B = 100.9T^{-3.57}$ for 10 μm outside BCP and $R_B = 69.2T^{-3.37}$ for 30 μm inside BCP surface.

As the thermal conductivity data for this host material isn't available, we are unable to separate the Kapitza term from the total thermal impedance. During the surface preparations, we can assume that the thermal conductivity of the niobium cavity remains unchanged, which allows us to calculate the change in Kapitza resistance as the surface modifications were made. Figure 4(b) shows the change in Kapitza resistance as a result of the surface preparations with initial condition being the nitrogen doping. The Kapitza resistance decreases after the nitrogen doped cavity is subjected to 7 μm EP of inner surface and it further reduces with additional 5μm EP. The Kapitza resistance increase after the cavity was subjected to light outside BCP and again decreases with an additional 30 μm inside BCP.

TD5

Cavity TD5 is a single cell cavity made from high purity ingot niobium from Tokyo Denkai. The cavity was also doped with nitrogen and rf measurements were carried out and are presented in ref. [14]. The cavity was heat treated at 800 °C for 3 hours followed by 20 minutes of exposure to nitrogen at pressure of ~25 mtorr at this temperature. The cavity's inner surface was electropolished to remove the inner surface layer and outer surface is removed by BCP. The results of measurement are shown in Fig. 5. Surprisingly the thermal impedance wasn't affected by EP or BCP. Once again, Kapitza resistance cannot be separated due to the unavailability of thermal conductivity data for the host material. The temperature dependence of thermal impedance shows a kink ~ 1.75K, where the phonon peak is expected to occur in thermal conductivity. The detail study on the effect of surface preparations on thermal impedance and the SRF cavity performance will be reported in future publications.

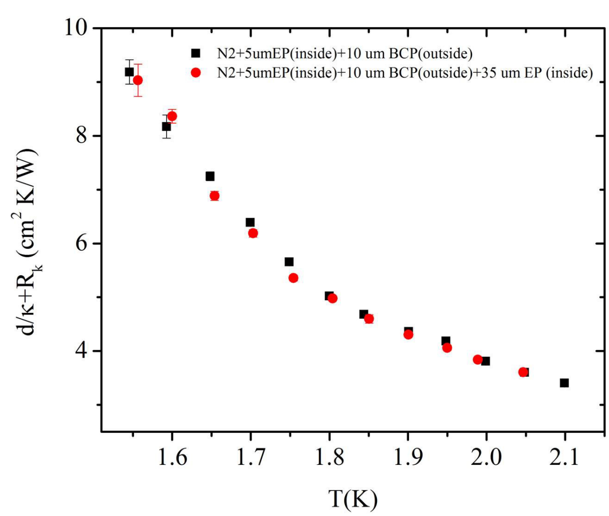

Figure 5: Results of the thermal impedance measurement on cavity TD5.

DISCUSSION

The experimental results show the effect of surface preparations on the thermal impedance, however its influence on the actual SRF cavities isn't fully understood. Bauer et al., [15] analyzed the cavities measurement data in terms of the thermal feedback model to analyze the medium and high field Q-slope as a result of non-linear BCS surface resistance. Low temperature baking on SRF cavities reduces the high field Q-slope significantly suggesting that the surface modification plays a role in lowering power dissipation (inner surface) due to the reduction in BCS related losses. More studies are needed to understand the effect of baking on Kapitza conductance. As mentioned, the temperature dependence of Kapitza resistance for cavity TC1N1 is consistent with the theoretical predictions and showed that, because of the high phonon peak in thermal conductivity the dominant term in heat transfer is Kapitza conductance. The cavity subjected to 15μm EP has the same temperature dependence of R_K as that of with an additional 30μm EP, and increase in R_K was observed after 13μm outside BCP. This shows that the increase in effective surface area doesn't necessarily reduce the R_K, but the surface impurity and crystal structure plays the significant role on R_K, consistent with previous experimental results on single crystal Nb [3].

As shown in Fig. 4(a), the thermal impedance has the highest values for the cavity doped with nitrogen. The doping of nitrogen caused some unwanted normal conducting precipitates on the surface of the cavity that may result in higher thermal impedance. After 7μm EP of inner surface the thermal impedance decreases and reduces further by an additional 5μm EP. It is evident that the surface doping results in the increase of thermal impedance consistent with the literature results [2, 3]. However, the thermal impedance increases as outside surface of cavity is subjected to 10μm BCP. The studies on effect of outside BCP on rf performance are in progress. On further BCP of inside surface the thermal impedance reduces. The increase in thermal impedance after 10μm BCP may be due to the increase in surface roughness as shown on single crystal Nb samples [3]. The reduction in thermal impedance observed with an additional 30μm inside BCP may be due to the removal of remaining nitrogen present after the 12μm EP. More experiments are planned to further understand the effect of surface impurities and surface roughness on thermal impedance.

The measurements on TD5 cavity showed little effect of outside BCP and inside EP on the thermal impedance, even though the cavity's rf performances are significantly different [14]. The thermal impedance has lower magnitude compared to the cavities TC1N1 and CBMM-A4, possibly due to the higher thermal conductivity (high RRR) of the bulk Nb. Further experiments are planned to modify the surface and measure the thermal impedance and rf performance.

The thermal conductance and Kapitza conductance have combied effect for the efficient heat transport in SRF cavities. The increasing thermal conductivity (higher RRR) of the material makes the Kapitza conductance the dominating

ISBN 978-3-95450-178-6

factor for efficient heat transfer. In other words, cavities made from higher RRR material not necessarily make the SRF cavity thermally stable against thermal quench. The current measurements give the average effect of the heat transfer across the cavity wall, however most of the time the cavity has localized quench sites due to the presence of defects and imperfections.

The thermal conductivity of SRF material in superfluid He temperature is largely influenced by the process typically applied during the cavity fabrication process. The mechanical deformations, impurities inclusion, material doping and crystal structure significantly reduce the thermal conductivity as well as the reduction of the phonon peak. On the other hand, high temperature heat treatment and bigger crystal grain increases the thermal conductivity as well as the phonon peak.

The Kapitza resistance is much more complicated to understand as it is related to the interface between the solid Nb and superfluid helium. Simple temperature dependence of Kapitza resistance is proportional to T^{-3} corresponds to the phonon heat capacity, however the experimental results vary widely. There exist two theoretical models to understand the Kapitza resistance at the boundary of Nb and superfluid helium, namely the acoustic mismatch model (smooth surface) and diffuse mismatch model (rough surface), based on the phonon transport at the boundary [10]. The SRF cavities have neither the perfectly smooth nor the rough surfaces, the measured Kaptiza resistance can be qualitatively explained within these two theoretical models.

SUMMARY AND FUTURE WORKS

We have measured the thermal impedance of SRF niobium cavities subjected to several surface preparations. The results show the influence of surface preparations on the thermal impedance. The effective heat transfer across the cavity wall during the cavity operation is influenced by both the material properties (thermal conductivity) as well as the surface perperations (Kapitza conductance). For SRF cavities made from high thermal conductivity niobium, the Kapitza conductance plays the significant role as breakdown field is assumed to be proportional to $R_K^{-1/2}$. Palmieri et al., [5] showed that the modification of outer surface via anodization resulted in the increase in quality factor as well as the breakdown field. Further experiments are planned to better understand the effect of surface perperations on thermal impedance on both fine grain and large grain SRF cavities and their rf performances.

ACKNOWLEDGMENT

We would like to acknowledge J. Follkie, A. Anderson, C. Johnson, T. Harris, P. Kushnick, D. Forehand, M. Morrone, S. Dutton and T. Goodman at Jefferson Lab for helping with EP, BCP, HT, cryogenic support and instrumentations.

REFERENCES

[1] A. Gurevich, Physica C **441**, 38 (2006).

[2] J. Amrit and M.X. Francios, J. Low Temp. Phys. **119**, 27 (2000).

[3] J. Amrit and C. Z. Antonie, Phys. Rev. ST Accel. Beams **13**, 023201 (2010).

[4] S. Bousson *etal*., Proc. of SRF99, Santa Fe, New Mexico, USA (1999), paper:TUP028.

[5] V. Palmieri, A. A. Rossi, S. Y. Stark, and R. Vaglio, Supercond. Sci. Technol. **27**, 085004 (2014).

[6] E. D. Marquardt, J. P. Le, and R. Radebaugh, Proc. of 11 International Cryocooler conference, Keystone, CO (2000).

[7] C. E. Chase, Phys. Rev. **127**, 361 (1962).

[8] H. Lengelar *etal*., Proc. of Applied Superconductivity Conference, San Diego, CA (1984).

[9] P. Dhakal *etal*., Proc. of SRF 11, Chicago, USA (2011), paper: TUPO057.

[10] E. T. Swartz and R. O. Pohl, Rev. Mod. Phys. **61**, 605 (1989).

[11] A Grassellino *etal*., Supercond. Sci. Technol. **26**, 102001, (2013).

[12] P. Dhakal *etal*., IEEE Transactions of Applied Superconductivity 25, 3500104 (2015).

[13] P. Dhakal *etal*., Proc. of IPAC15, Richmond VA (2015), paper: WEPWI009.

[14] A. Palczewski *etal*., Proc. of SRF15, Wristler, Canada (2015), paper: MOPB039.

[15] P. Bauer *etal*., Physica C **441**, 51 (2006).